

### Farey-Fraction Frequency Modulation in the Neuronlike Output of Silicon *p-i-n* Diodes at 4.2 K

D. D. Coon, S. N. Ma, and A. G. U. Perera

Department of Physics, University of Pittsburgh, Pittsburgh, Pennsylvania 15260

(Received 21 July 1986)

The first temporal analysis of spontaneous pulsing of dc-biased, *p-i-n* diodes in *RC* circuits is reported. Time intervals  $T_n$  between successive pulses in spike trains with durations up to 30 h are analyzed as a function of  $n$ . Temporal patterns depend on bias voltage and are characterized by symmetric sets of Farey-fraction frequencies associated with remarkably narrow peaks in power spectra. Resolution permitted identification of 115 of the 129 Farey fractions with period  $\leq 40$ . A rule involving fractions appearing in this system and other nonlinear systems is proposed.

PACS numbers: 73.40.Lq, 05.40.+j, 87.30.Ew

We report here the first temporal analysis of a nonlinear system consisting of a forward-dc-biased, liquid-helium-cooled, *p-i-n* ( $p^+ - n - n^+$ ) diode in series with an *RC* load impedance<sup>1,2</sup> as shown in Fig. 1. This circuit spontaneously generates a continuing sequence of fast pulses<sup>1-4</sup> similar to a neuron spike train. Our experiments show that these neuronlike spike trains can exhibit frequency modulation characterized by narrow power-spectrum peaks which proliferate in the manner of a Cantor set as the bias voltage is decreased.

The diode transient behavior is neuronlike in the sense that neurons exhibit all-or-nothing transients involving temporary switching from the normal, polarized, low-conductance state of the axon membrane to a depolarized, conducting state.<sup>5</sup> Successive pulses are *nearly identical* so that information can be effectively conveyed only via *modulation of time intervals between pulses*. The large pulse height ( $\approx 9$  V in the work reported here) and the fast rise time (80 ns) give a high slew rate (0.1 V/ns) providing a very favorable experimental circumstance for precision timing of intervals between pulses ( $T_n$  with  $n=1,2,3,\dots$ ).  $T_n$  from about 100 ns to 8 h have been observed.

Spike-train generation is not fully understood, but some key aspects appear to be as follows. At 4.2 K the impurities (phosphorus donors) in the *i* region ( $N_P \sim 10^{13} \text{ cm}^{-3}$ ) act as traps with long ( $> 10^5$  s) lifetimes.<sup>6</sup> Between pulses, a small forward current density causes these traps to be slowly depleted by impact ionization, e.g.,  $e^- + P \rightarrow P^+ + e^- + e^-$  with the electrons being swept away by the field in the *i* region (see Fig. 1). This results in an increasing, *positive* space-charge density  $\rho$  and hence an increasing field near the *n-i* interface. The space-charge buildup is described by  $d\rho/dt = n\sigma j$ , where  $\sigma$  is the impact ionization cross section and  $n$  is the concentration of un-ionized traps. From Gauss's law, the field  $F$  at the *n-i* interface is found to be

$$F = \frac{1}{D}(V - V_0) + \frac{1}{D\epsilon} \int_0^D x\rho(x) dx, \tag{1}$$

where  $V$  is the voltage across the diode,  $D$  is the *i*-region thickness (0.2 mm), and  $V_0 = 1.1$  V accounts for the

Fermi-level difference between the *p* and *n* impurity bands. Impact ionization can proceed very slowly at first because injection of electrons into the *i* region is inhibited by an interfacial work function  $\Delta$  at the *n-i* interface. For a typical  $\Delta$  of 29 meV<sup>7,8</sup> obtained from temperature dependence of dc current, the inhibition  $\exp(-\Delta/kT)$  at 4.2 K can be substantial. However, the increasing field  $F$  reduces the barrier height and enhances electron injection.<sup>7,9</sup> A simple model for barrier-height reduction is  $\Delta \rightarrow \Delta - eFd$  where  $d$  is an interface thickness parameter.<sup>7</sup> The Richardson-Dushman equation for the injec-

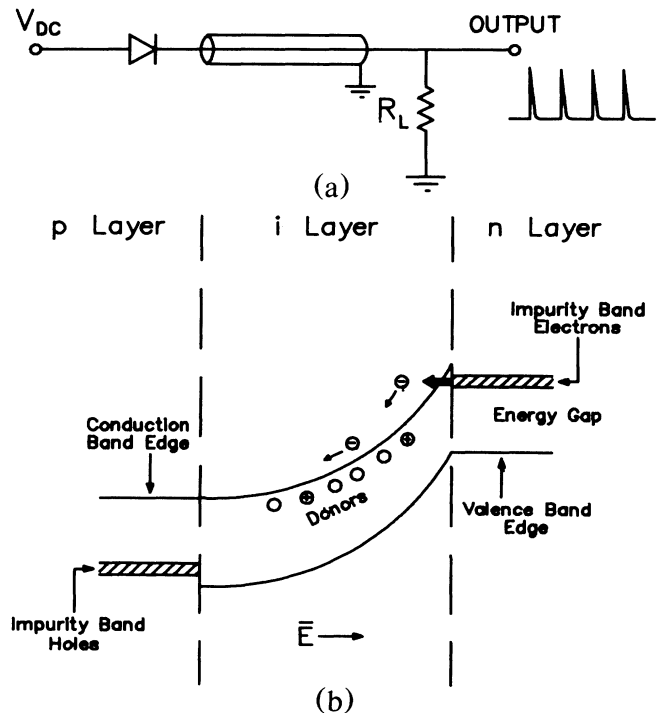


FIG. 1. (a) Circuit diagram showing the experimental set-up. The load impedance consists of  $R = 50$  K and a cable capacitance  $C = 200$  pF. (b) Band diagram for the forward-biased *p-i-n* diode. Impact ionization causes the *i*-region space charge and band bending.

tion current density<sup>7</sup> becomes

$$j = A^* T^2 e^{-(\Delta - edF)/kT}, \quad (2)$$

where  $A^*$  is the effective Richardson constant.<sup>10</sup> As an illustrative model of the polarized, low-conductance interpulse interval, we (a) ignore recapture, the charge density of transiting electrons, and the effect of the load impedance so that  $V = V_{dc}$ , (b) take  $\sigma$  to be constant, (c) assume that changes in  $n$  are small compared to  $n$ , and (d) combine the above equations to obtain  $j(t) = j(0)/(1 - t/T_0)$  where

$$j(0) = A^* T^2 \exp[-\Delta + (ed/D)(V - V_0)]/kT$$

and  $T_0 = 2ekT/edDn\sigma j(0)$  is the interpulse time interval. A virtue of this simplified model is that one can see how the system can evolve slowly for a long time as a result of small  $j(0)$  after which the injected current can increase rapidly. For example,  $j$  has been observed to remain near  $j(0) \sim 0.1$  pA/mm<sup>2</sup> for 180 s and then rapidly rise by a factor of  $10^{11}$  to  $j \sim 10$  mA/mm<sup>2</sup>. The current pulse charges  $C$  and the sudden voltage drop across  $C$  abruptly depolarizes the diode ( $V \rightarrow V_{dc} - 9$  V) and shuts off the large current. During depolarization, the low field favors trapping and the large electron current tends to neutralize the positive space charge.<sup>6</sup> Subsequent discharge of  $C$  through  $R$  resets the initial diode bias, i.e.,  $V = V_{dc}$ . Shutoff and prompt resetting are achieved with  $RC$  (10  $\mu$ s here) longer than the rise time ( $\sim 80$  ns) but significantly shorter than the  $T_n$ 's studied here (35 ms to 180 s). Order-of-magnitude  $T_0$  estimates based<sup>11,12</sup> on  $\sigma \sim 10^{-13}$  cm<sup>2</sup>,  $d \sim 0.3$   $\mu$ m, and  $D \sim 200$   $\mu$ m agree with observed  $T_n$ 's. Other evidence for the space-charge buildup mechanism has been obtained from experiments in which pulse rates were enhanced by infrared photoionization of  $i$ -region donors.<sup>1,2,4</sup> The repetitive cycle of slow space-charge buildup followed by a fast neutralizing pulse has qualitative similarities with integrate-and-fire, relaxation-oscillator-type models.<sup>13,14</sup> If every injection pulse caused complete neutralization of the space charge then the initial conditions for each cycle would be the same and we would expect equal  $T_n$ 's. However, the observed temporal patterns are more complex. We attribute this complexity to incomplete neutralization which permits the space charge to retain information about previous time intervals.

Spontaneous spike-train generation has been observed with about fifteen diodes. Bias-voltage ranges can be found which produce nearly periodic patterns, with period 2 through period 9 being frequently observed. Here we examine the firing pattern as a function of dc bias voltage for a diode which exhibits strong period-2 interpulse interval modulation (frequency modulation). This interval modulation pattern parallels the period-2 large-small  $LSLSLS \dots$  amplitude modulation pattern

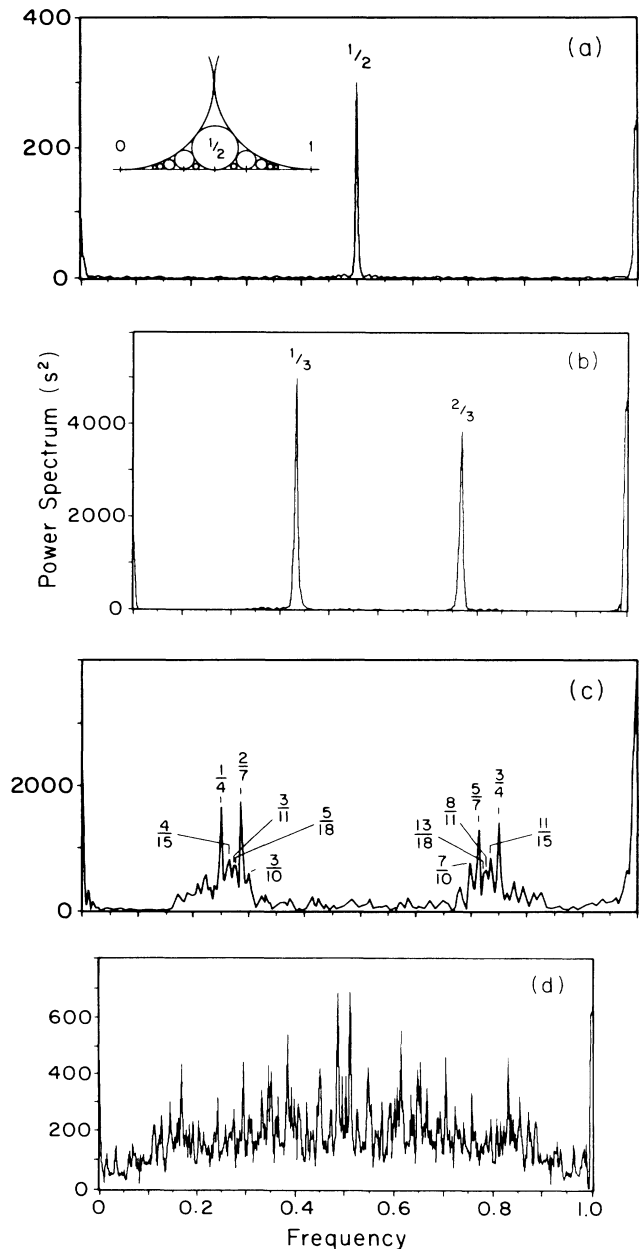


FIG. 2. Power spectra with unity on the horizontal frequency scale corresponding to  $f_{max} = 1/2$  or period 2. (a) Spectrum obtained from 1024 interpulse time intervals at 12.35 V bias showing Farey fractions 0/1, 1/2, 1/1. Inset: Ford circles, which are an infinite set of tangent circles clustering on the interval (0,1). Lines joining centers of adjacent circles form a graph like that in Fig. 3. (b) Spectrum at 12.00 V showing peaks at 0/1, 1/3, 2/3, 1/1. The 1/3 and 2/3 components are indicative of period 6. The peak at  $f=1$  is scaled down by a factor of 10. (c) Spectrum at 11.91 V showing peaks at 0/1, 1/4, 4/15, 3/11, 5/18, 2/7, 3/10, 7/10, 5/7, 13/18, 8/11, 11/15, 3/4, 1/1. (d) Spectrum obtained from 6144 interpulse time intervals at 11.55 V. Identification of 91 peaks at Farey fraction of order 20 is given in Fig. 3. The peak at  $f=1$  is scaled down by a factor of 1000.

in the Belousov-Zhabotinskii (BZ) reaction,<sup>15</sup> which also involves a dc parameter, the flow rate.

The period-2 patterns we observe consist of alternating long ( $L$ ) and short ( $S$ ), i.e.,  $LSLS\dots$ , interpulse time intervals. Examples of  $L$  and  $S$  are 180 and 45 s corresponding to  $j(0)\sim 0.1$  pA/mm<sup>2</sup> and  $j(0)\sim 0.4$  pA/mm<sup>2</sup>. Closer inspection reveals subcategories, e.g.,  $L_1S_1L_2S_2$ , as well as some intermittency.<sup>16</sup> Autocorrelation functions display correlations up to  $n=3000$  (24 h) but typically with intervening nodes of low correlation. We study  $T_n$  as a function of  $n$  and consider modulation frequencies ranging from zero (for  $LLLL\dots$  and  $SSSS\dots$ ) to  $f_{\max}=1/2$  for a period-2 sequence. An  $LSLS\dots$  sequence has frequency components  $f=0$  and  $f=1$ , in units of  $f_{\max}$ .

Pulses were monitored on a 200-MHz oscilloscope and supplied to the trigger input of a CAMAC microcomputer system which recorded the time of arrival (TOA) of every pulse. A fast pulse counter was checked against the number of TOA's recorded. Power spectra were obtained from  $T_n$ 's by a fast Fourier transform program. Spectral resolution and overall hardware and software performance were checked with pulse patterns from a Wavetek arbitrary waveform generator. Power spectra obtained from  $T_n$  as a function of  $n$  are shown in Fig. 2 where the horizontal scale corresponds to frequency  $f$  as a fraction of  $f_{\max}$ . The spectra show peaks at  $f=p/q$  (in units of  $f_{\max}$ ) where  $p/q$  represents a fraction with  $p$  and  $q$  being coprime integers. The set  $f_N$  of all such fractions with  $0\leq p\leq q\leq N$  is called a Farey sequence of order  $N$ .<sup>17,18</sup> Each set  $F_N$  is symmetric under  $f\rightarrow 1-f$  and this symmetry is apparent in the power spectra. Except for  $f\rightarrow 1-f$  symmetry there is no correlation between harmonics, e.g., in a given spectrum  $2/7$  and  $5/7$  can be much larger than  $1/7$ ,  $3/7$ ,  $4/7$ , and  $6/7$ . Symmetry is not apparent in other experimental work.<sup>15,19</sup>

In general, a power spectrum at a particular bias voltage does not display all Farey fractions of some order  $N$  but only a subset of  $f_N$ . We have surveyed sets of power spectra to see how many members of  $F_{20}$  (period  $\leq 40$ ) can be found. The survey was not exhaustive in terms of a large number of small increments in bias voltage because typical high-resolution power spectra require a 30-h run at 4.2 K. Order 20 was selected on the basis of power-spectrum resolution, which was found to be about 0.003 full width at half maximum (FWHM) in tests with the Wavetek. High-resolution power-spectrum frequency intervals were about 0.002. The average spacing between the 129  $F_{20}$  fractions is about 0.008 although spacings as small as 0.0026 do occur. For an equal number of pulses (6144) from the diode and the Wavetek, the widths of Farey-fraction peaks were found to be comparable to the widths of Wavetek peaks. Thus, the intrinsic experimental peak widths are remarkably small ( $< 0.003$  FWHM). Altogether 115 of the 129 fractions of  $f_{20}$  were found in our survey. A more exhaustive

search could well reveal all 129. Deviations of 115 measured peak positions from Farey fractions show no disagreement with a Gaussian distribution with 0.003 FWHM and a standard deviation of 0.0013. This indicates that deviations may simply be related to power-spectrum resolution.

The quantity  $|pl - qk|$  is called the modularity of  $p/q$  and  $k/l$ . When a sequence  $f_N$  is ordered by magnitude, consecutive fractions  $p/q$  and  $k/l$  satisfy the unimodularity condition<sup>13</sup>  $|pl - qk| = 1$ . We refer to this sequence property as sequential unimodularity. Lines between  $F_{20}$  fractions in Fig. 3 indicate unimodular relationships. Figure 3 illustrates that there are *more unimodular relationships* between fractions in a set  $F_N$  than exist among adjacent<sup>20</sup> fractions in  $F_N$  as a numerically ordered sequence. An elegant way to illustrate all unimodular relationships is with Ford circles<sup>17</sup> (see Fig. 2 inset). Each Farey fraction  $p/q$  corresponds to a Ford circle of radius  $1/2q^2$  centered at  $x=p/q$ ,  $y=1/2q^2$ . Ford circles associated with  $p/q$  and  $k/l$  are tangent if and only if  $|pl - qk| = 1$ . Thus, the Ford-circle construct endows Farey fractions with a plane-geometry nearest-neighbor (2D adjacency) concept like the rule for connectedness of stones on a Go board.

The  $f=0$  and  $f=1$  components of  $LSLS\dots$  correspond to the  $F_1$  fractions  $0/1$  and  $2/1$ . In Fig. 2 we observe peaks at  $F_2$  fractions  $0/1$ ,  $1/2$ ,  $1/1$  and, at a lower bias voltage,  $F_3$  peaks corresponding to  $0/1$ ,  $1/3$ ,  $2/3$ ,  $1/1$ , with  $1/2$  missing. The absence of  $1/2$  in the latter sequence introduces a sequential "unimodularity gap" between  $1/3$  and  $2/3$ , i.e.,  $|pl - qk| = 3$ . Maseiko and Swinney, in their study of transition sequences in the BZ reaction, observed such gaps as did Allen<sup>13</sup> in a tabulation of Harmon's artificial neuron results.<sup>19</sup> We find that sequences associated with peaks such as those in Fig. 2 are *typically unimodular with occasional gaps*. Additional illustrative spectral sequences are  $1/4$ ,  $4/15$ ,

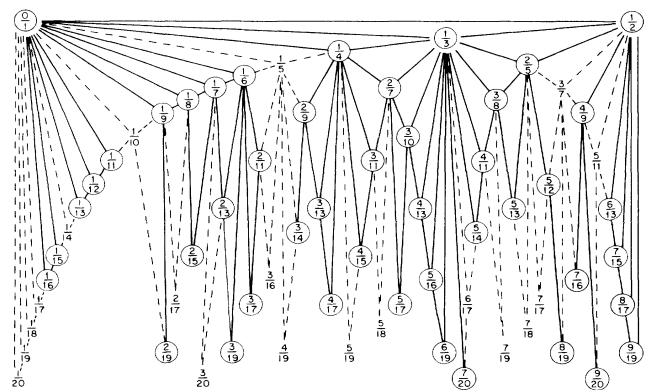


FIG. 3. Farey fractions of order 20 with  $f\leq 1/2$ . Fractions corresponding to peaks in Fig. 2(d) are circled and connectedness is emphasized by solid lines. Because of  $f\rightarrow 1-f$  symmetry, only fractions on the interval  $(0, 1/2)$  are displayed.

3/11, 2/7, 3/10, 8/25, 1/3, 4/11, with modularity 1, 1, 1, 1, 5, 1, 1, and 3/14, 2/9, 3/13, 4/17, 6/25, 1/4, 7/27, with modularity 1, 1, 1, 2, 1, 1. One is initially tempted to feel that such gaps indicate that some peak has been missed experimentally. The feeling that something is missing is reflected in the papers of Allen<sup>13</sup> and Maselko and Swinney.<sup>15</sup> However, we suggest an alternative view that experimental unimodularity may be associated with a 2D connectedness rule rather than sequential unimodularity. This permits the observed sequence gaps to be bridged by unimodular relationships between fractions which are adjacent in the 2D graph or Ford-circle construct. Thus, the unimodularity gap in the 0/1, 1/3, 2/3, 1/1 spectrum is bridged by the unimodular relationship between 0/1 and 1/1. Note that removal of 1/2 does not spoil the connectedness of the remaining set of Ford circles in Fig. 2. The peaks in Fig. 2(d) provide an example of a connected set of 91 fractions with the connectedness illustrated in Fig. 3. We find that the 2D connectedness rule also bridges the sequential unimodularity gaps in the ordered sequence of phase-locking ratios<sup>13</sup> for Harmon's artificial neurons.<sup>19</sup> BZ-reaction periodic-state transition sequences<sup>15</sup> also support the 2D connectedness rule.

Examination of 191 peaks in three power spectra revealed 41 sequential (1D) unimodularity gaps but only two exceptions to the 2D connectedness rule. Rare exceptions might be associated with the tails of the measurement distribution discussed above or obscuration of peaks by stronger neighboring peaks. One exception involves peaks at 3/17 and 4/23, a unimodularly coupled pair which, for a particular bias voltage, are topologically disconnected from the main body of peak structure by the absence of unimodularly related peaks at 1/6 and 2/11. This exception illustrates a *general rule*: Absence of two unimodularly related Farey fractions can result in 2D disconnectedness of a set of Farey fractions. This is because removal of *any two adjacent Ford circles* other than the exterior circles (0/1 and 1/1) divides the set of all Ford circles into two disconnected subsets. This remarkable property implies that disconnected sets of peaks could easily occur so that accidental agreement with the 2D rule seemed highly unlikely.

We conclude that we are dealing with a nonlinear system whose modes are associated with the numerology and topology of Farey fractions. Richer spectra, typically at lower bias voltages, involve higher-order Farey fractions and an impressive set of unimodular relationships indicative of 2D connectedness. Equally striking are the symmetry about  $f=1/2$  and narrow widths which permit large numbers of peaks to be resolved. In recent years, theories have encountered Farey fractions in the analysis of very diverse physical and mathematical phenomena including circle maps, Cantor sets, and

devil's staircases.<sup>18,21-27</sup> However, there is as yet no quantitative theory which explains the appearance of Farey fractions in the physical system studied here.

The authors have benefitted from conversations with R. Devaty. This work was supported in part by the U.S. National Science Foundation under Grant No. ECS-8603075 and the Department of Energy under Contract No. DE-AC02-80ER10667.

<sup>1</sup>D. D. Coon and S. D. Gunapala, J. Appl. Phys. **57**, 5525 (1985).

<sup>2</sup>D. D. Coon and A. G. U. Perera, Solid State Electron. **29**, 929 (1986).

<sup>3</sup>L. H. De Vaux, U.S. Patent No. 3 466 448.

<sup>4</sup>D. D. Coon and A. G. U. Perera, Int. J. Infrared and Millimeter Waves **7**, 1571 (1986).

<sup>5</sup>B. Katz, *Nerve, Muscle, and Synapse* (McGraw-Hill, New York, 1966), p. 34.

<sup>6</sup>J. R. Banavar, D. D. Coon, and G. E. Derkits, Phys. Rev. Lett. **41**, 567 (1978).

<sup>7</sup>Y. N. Yang, D. D. Coon, and P. F. Shepard, Appl. Phys. Lett. **45**, 752 (1984).

<sup>8</sup>D. Schechter, J. Appl. Phys. **61**(2), 591 (1987).

<sup>9</sup>W. Schottky, Z. Phys. **14**, 63 (1923).

<sup>10</sup>S. M. Sze, *Physics of Semiconductor Devices* (Wiley, New York, 1969).

<sup>11</sup>A. G. Milnes, *Deep Impurities in Semiconductors* (Wiley, New York, 1973), p. 379.

<sup>12</sup>N. F. Mott, *Metal-Insulator Transitions* (Barnes and Noble, New York, 1974).

<sup>13</sup>T. Allen, Physica (Amsterdam) **6D**, 305 (1983).

<sup>14</sup>L. Glass, C. Graves, G. A. Petrillo, and M. C. Mackey, J. Theor. Biol. **86**, 455 (1980).

<sup>15</sup>J. Maselko and H. L. Swinney, Phys. Scr. **T9**, 35 (1985).

<sup>16</sup>J. Hirsch, B. Huberman, and D. Scalapino, Phys. Rev. A **25**, 519 (1982).

<sup>17</sup>H. Rademacher, *Lectures on Elementary Number Theory* (R. E. Krieger, Huntington, New York, 1977).

<sup>18</sup>P. Bak, T. Bohr, and M. H. Jensen, Phys. Scr. **T9**, 50 (1985).

<sup>19</sup>L. D. Harmon, Kybernetik **1**, 89 (1961).

<sup>20</sup>D. L. Gonzalez and O. Piro, Phys. Rev. Lett. **50**, 870 (1983).

<sup>21</sup>M. Feigenbaum, "Renormalization of the Farey Map and Universal Mode Locking" (to be published).

<sup>22</sup>P. Cvitanovic, M. H. Jensen, L. P. Kadanoff, and I. Procaccia, Phys. Rev. Lett. **55**, 343 (1985).

<sup>23</sup>L. Glass and R. Perez, Phys. Rev. Lett. **48**, 1772 (1982).

<sup>24</sup>S. Ostlund, D. Rand, J. Sethna, and E. Siggia, Physica (Amsterdam) **8D**, 303 (1983).

<sup>25</sup>S. Sato, Kybernetik **11**, 208 (1972).

<sup>26</sup>S. Aubry, F. Axel, and F. Vallet, J. Phys. C **18**, 753 (1985).

<sup>27</sup>R. S. Mackay, J. D. Meiss, and I. C. Percival, Physica (Amsterdam) **13D**, 55 (1984).